# Rate Constants and Products of the OH Reaction with Isoprene-Derived Epoxides

Michael I. Jacobs, Adam I. Darer, and Matthew J. Elrod*

Department of Chemistry and Biochemistry, Oberlin College, 119 Woodland Street, Oberlin, Ohio 44074, United States

Ⓢ *Supporting Information*

ABSTRACT: Recent laboratory and field work has shown that isoprene-derived epoxides (IEPOX) are crucial intermediates that can explain the existence of a variety of compounds found in ambient secondary organic aerosol (SOA). However, IEPOX species are also able to undergo gas phase oxidation, which competes with the aerosol phase processing of IEPOX. In order to better quantify the atmospheric fate of IEPOX, the gas phase OH reaction rate constants and product formation mechanisms have been determined using a flow tube chemical ionization mass spectrometry technique. The new OH rate constants are generally larger than previous estimations and some features of the product mechanism are well predicted by the Master Chemical Mechanism Version 3.2 (MCM v3.2), while other features are at odds with MCM v3.2. Using a previously proposed kinetic model for the quantitative prediction of the atmospheric fate of IEPOX, it is found that gas phase OH reaction is an even more dominant fate for chemical processing of IEPOX than previously suggested. The present results suggest that aerosol phase processing of IEPOX will be competitive with gas phase OH oxidation only under SOA conditions of high liquid water content and low pH.
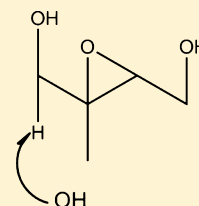
INTRODUCTION

Secondary organic aerosol (SOA) plays a critical role in issues such as air pollution and climate change.[1-3] Isoprene (2-methyl-1,3-butadiene) is the largest source of nonmethane hydrocarbon emitted into the atmosphere,[4] and both laboratory and field measurements have confirmed the importance of isoprene oxidation in the production of SOA. Many chemically distinct compounds possessing the isoprene carbon backbone, including species with alcohol, ether, sulfate, and/or nitrate functional groups, have now been identified on ambient SOA.[5-13] Paulot et al. identified gas phase intermediates (3-methyl-3,4-epoxy-1,2-butanediol, IEPOX-1, and 2-methyl-2,3-epoxy-1,4-butanediol, IEPOX-4) produced from the photo-oxidation of isoprene in an environmental chamber under low NO_x conditions.[14] Subsequent laboratory[13,15-18] and field work[5,18-21] has demonstrated that aerosol phase nucleophilic reactions involving these IEPOX species on SOA are kinetically facile mechanisms for the formation of the alcohol, sulfate, and nitrate-containing species found on ambient SOA.

While the aerosol phase nucleophilic reaction mechanism involving IEPOX is undoubtedly an important atmospheric fate for IEPOX compounds, further gas phase oxidation of IEPOX compounds is also possible and must be understood and quantified in order to adequately model the atmospheric chemical processing of isoprene. The atmospheric fate of a generic IEPOX compound was modeled by Eddingsaas et al. by using estimates for both the gas phase OH radical-initiated photooxidation and the aerosol phase hydrolysis rate constants.[22] The model suggested gas phase oxidation is the main fate of IEPOX, except under conditions of high aerosol liquid water content and low aerosol pH. However, since both the gas and aerosol phase rate constants used in that study were estimated values, the quantitative results of that study were of

unknown accuracy. Since the publication of the Eddingsaas study, our laboratory has measured and reported the hydrolysis rate constants for both IEPOX-1 and IEPOX-4,[17] so the only key piece of information missing to allow a more accurate modeling of IEPOX's atmospheric fate is knowledge of the gas phase OH rate constant for these compounds.

In the present study, the two IEPOX compounds observed by Paulot et al. (IEPOX-1 and IEPOX-4)[14] are synthesized and, for the first time, their gas phase OH oxidation rate constants have been determined using a flow tube chemical ionization mass spectrometry relative rate technique. Furthermore, a product study for both IEPOX compounds was performed to determine the mechanism by which IEPOX-1 and IEPOX-4 undergo OH-initiated gas phase oxidation. With the results from the new gas phase rate constant experiments and with the aerosol phase hydrolysis rate constants previously measured in our lab,[17] the Eddingsaas et al. model[22] is refined to provide a more accurate quantitative prediction of the atmospheric fate of these IEPOX compounds.

EXPERIMENTAL SECTION

Syntheses of IEPOX-1 and IEPOX-4. The methods used in the syntheses of IEPOX-1 and IEPOX-4 were similar to those already reported by our laboratory,[17] and were based, in part, on previously published procedures.[23-25] The full details of the methods are given in the Supporting Information (SI).

Flow Tube Apparatus. The setup of the flow tube system was similar to a recent study reported by our laboratory.[26] The

full details of the flow tube system and an experimental schematic are given in the SI.

OH Source. The F + H$_2$O OH-source utilizes the microwave discharge-initiated dissociation of CF$_4$, followed by reaction with H$_2$O:

$$CF_4 \rightarrow xF + CF_{4-x} \tag{1}$$

$$F + H_2O \rightarrow OH + HF \tag{2}$$

A 4.0% mixture of CF$_4$/ultra high purity He was passed through a microwave discharge, produced by a Beenakker cavity operating at 50 W, to create fluorine atoms (reaction 1). The fluorine atoms were then injected into the flow tube side arm and mixed with H$_2$O/He, produced by bubbling 12 mL min^{-1} He through a trap filled with H$_2$O to produce OH radicals (reaction 2). Because H$_2$O is in great excess ([H$_2$O] $\sim$ 2 × 10^{14} molecules cm^{-3}) and the F + H$_2$O reaction is very fast (1.4 × 10^{-11} cm^{-3} molecule^{-1} s^{-2}),[27] the OH-producing reaction has a very short lifetime of about 0.4 ms, thus ensuring that all F atoms are quickly consumed. For similar experimental conditions,[26] we have estimated that this source leads to maximum OH concentrations of about 5 × 10^{11} molecules cm^{-3}.

CIMS Detection. The chemical ionization reagent ions were produced using a commercial polonium-210 α-particle emitting ionization source consisting of a hollow cylindrical (69 by 12.7 mm) aluminum body with 10 mCi (3.7 × 10^8 disintegrations s^{-1}) of polonium-210 coated on the interior walls. All oxygenated organic species were detected using a proton transfer (PTR-CIMS) scheme. The H$^+$(H$_2$O)$_n$ ions were produced by passing a large O$_2$ flow (7 STP L min^{-1}) through the ionization source with H$_2$O impurities being sufficiently abundant to produce an adequate amount of reagent ions. The dominant chemical reagent ion was H$^+$(H$_2$O)$_4$ and the predominant proton transfer species detected were the protonated (and partially hydrated) analogs of the neutral precursor oxygenated organic compounds. For both the OH rate constant and product studies, all ions (MH$^+$(H$_2$O)$_n$) assigned to a particular species (M) were summed and normalized to the total reagent ion signal (H$^+$(H$_2$O)$_n$) for that particular experiment in order to determine a CIMS signal that was not dependent on the ion hydrate distribution nor on the total ion signal.

OH Rate Constant Measurement Method. Attempts to carry out absolute OH reaction rate constant measurements (via measurements of the decay of OH in the presence of excess IEPOX concentrations) were not successful. While OH can be directly detected with negative-mode CIMS via the OH$^-$ ion,[28] which is produced from the charge transfer reaction of the reagent ion SF$_6^-$ with OH, OH$^-$ itself is a very reactive ion species. In particular, even though the ion−molecule reaction times in the CI region of the instrument were much shorter than the neutral reaction times in the flow tube, we found that ionic OH$^-$ reacted more quickly with the epoxides than did neutral OH, thus preventing the use of the OH$^-$ species as a proxy for the concentration of neutral OH. This finding is consistent with an earlier kinetics study of the reaction of OH$^-$ with 1,2-epoxypropane which found that the rate constant for this process is near the collision-limited value.[29] A previous CIMS-based kinetics study has also noted the difficulty in using OH$^-$ as a proxy for neutral OH concentrations.[30]

Instead, a relative rate constant measurement was performed by monitoring the decay of both the epoxide and a competitor

species in the presence of OH radicals.[31] Previous investigations using the OH source have shown that both OH and HO$_2$ radicals are produced under the present experimental conditions.[32] However, HO$_2$ reactions with the IEPOX and competitor compounds are likely to be much slower than the OH reactions, and it is reasonable to assume that both compounds react only with OH radicals under the experimental conditions,

$$epoxide + OH \rightarrow products \tag{3}$$

$$competitor + OH \rightarrow products \tag{4}$$
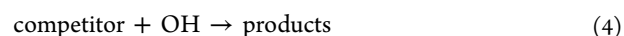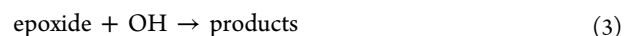
It can be shown that

$$\ln \frac{[epoxide]_{t,0}}{[epoxide]_{t,OH}} = \frac{k_3}{k_4} \ln \frac{[competitor]_{t,0}}{[competitor]_{t,OH}} \tag{5}$$

where [epoxide]$_{t,0}$ and [competitor]$_{t,0}$ are the concentration of the epoxide and the competitor species in the absence of OH radicals at time t, and [epoxide]$_{t,OH}$ and [competitor]$_{t,OH}$ are the concentrations of the epoxide and competitor species in the presence of OH radicals at time t, and k_3 and k_4 are the rate constants for reactions 3 and 4, respectively. Therefore, a plot of ln([epoxide]$_{t,0}$/[epoxide]$_{t,OH}$) vs ln([competitor]$_{t,0}$/[competitor]$_{t,OH}$), yields a slope equal to the ratio k_3/k_4. In order to the use this method to determine the OH + epoxide reaction rate constant, the relative changes in both the epoxide and competitor concentrations with respect to OH exposure must be measured. The relative rate method does not require knowledge of either the absolute concentrations of the epoxide and competitor species (rather relative concentrations are required, which are assumed to be proportional to the CIMS signal), nor does it require knowledge of the absolute reaction time (which is a fixed quantity in eq 5). These features are important for the present experiments since the vapor pressures (needed to calculate the absolute concentrations in the flow tube) of the IEPOX species are not known and the flow tube was operated in the laminar-turbulent flow transition region (where there is not a straightforward relationship between the bulk flow velocity and the molecular velocities) in order to allow longer reaction times and more extensive loss of both the epoxide and the competitor species. In order to achieve different reaction conditions, both the reaction time (injector distance) and the epoxide and competitor concentrations were varied. Proton transfer CIMS (PTR-CIMS) was used to detect both the epoxides and the competitor species (which, like the epoxide species themselves, contained hydroxyl groups, which are excellent proton transfer targets). The ratio of concentrations with the OH source on and off was obtained by simply monitoring and comparing both the epoxide's and competitor species' signals with the OH source on and off. The competitors used were 2-methyl-2-propen-1-ol, 3-methyl-3-buten-1-ol and 3-methyl-2-buten-1-ol with OH rate constants of (9.2 ± 1.3) × 10^{-11}, (9.7 ± 1.8) × 10^{-11} and (1.50 ± 0.10) × 10^{-10} cm^3 molecules^{-1} s^{-1}, respectively.[33] From the competitors' known rate constants, their ratios were normalized to 3-methyl-3-buten-1-ol's OH rate constant by treating the competitors as competitors with each other. Thus the normalized signal can be calculated as follows:

$$\ln \frac{[\text{normalized competitor}]_{t,0}}{[\text{normalized competitor}]_{t,\text{OH}}}$$

$$= \frac{k_4}{k_4{}'} \ln \frac{[\text{reference competitor}]_{t,0}}{[\text{reference competitor}]_{t,\text{OH}}} \qquad (6)$$

Where $\ln([\text{normalized competitor}]_{t,0}/[\text{normalized competitor}]_{t,\text{OH}})$ is the value plotted against $\ln([\text{epoxide}]_{t,0}/[\text{epoxide}]_{t,\text{OH}})$, k_4 is the OH rate constant of 3-methyl-3-buten-1-ol and $k_4{}'$ is the rate constant of the competitor being normalized (the derivation of eq 6 is given in the SI). By normalizing the competitors' ratios, the data from each of the competitor experiments could be plotted on a single graph using eq 5 and be used to determine a single rate constant ratio from all data (this method also serves as an internal validation of the consistency of the results for the different competitor experiments). The isomer-specific IEPOX OH rate constant, k_3, was determined from the calculated slope value and the known competitor rate constant, k_4.

OH Oxidation Product Study. A PTR-CIMS-based study of the OH-epoxide reaction products was performed for both IEPOX-1 and IEPOX-4 in order to determine the mechanisms by which the OH radical reacts with each species. Relatively high concentrations of the epoxides (to aid in the identification of lower yield product species) were added to the flow system and mass spectra were collected with the OH source on and off. Comparison of these spectra showed which masses corresponded to products of the OH reaction. These particular masses were then quantitatively monitored with the OH source on and off. Similar measurements were made when excess NO ($>1 \times 10^{13}$ molecules cm^{-3}) was added to the flow system. In the former case, the observed products are likely formed by peroxy + peroxy (including hydroperoxy) radical reactions, while in the latter case the observed products are likely formed as a result of peroxy + NO reactions. By comparing the signal from one product to the combined signal from all of the products (and assuming equivalent PTR-CIMS response factors), the relative product ratios were determined. Chemical structures were assigned to each of the product masses and a mechanism was produced to rationalize the observed species.

RESULTS AND DISCUSSION

OH Rate Constant Determination. The OH rate constants were obtained via competition experiments, using 2-methyl-2-propen-1-ol, 3-methyl-3-buten-1-ol and 3-methyl-2-buten-1-ol as the competitors with known rate constants (these competitor compounds react with OH via an addition mechanism; however the rate constants are at their high pressure limit at 100 Torr).[33] The signals from the competitors and the epoxides were monitored with the OH source on and off. Because the competitors' ratios were normalized to 3-methyl-3-buten-1-ol's OH rate constant, all of the data for each epoxide were plotted on the same graph. The plot of $\ln([\text{IEPOX-1}]_{t,0}/[\text{IEPOX-1}]_{t,\text{OH}})$ vs $\ln([\text{normalized competitor}]_{t,0}/[\text{normalized competitor}]_{t,\text{OH}})$ is shown in Figure 1. The slope of the best fit line in Figure 1, 0.363 ± 0.032, which is equivalent to the ratio of IEPOX-1's OH rate constant to 3-methyl-3-buten-1-ol's OH rate constant (k_3/k_4). Using the competitor's, 3-methyl-3-buten-1-ol, known OH rate constant, the IEPOX-1 + OH rate constant was calculated to be $3.52 \pm 0.72 \times 10^{-11}$ cm^3 molecule^{-1} s^{-1} (one standard deviation error, which includes contributions from both the relative rate constant uncertainty k_3/k_4 and uncertainty in the absolute
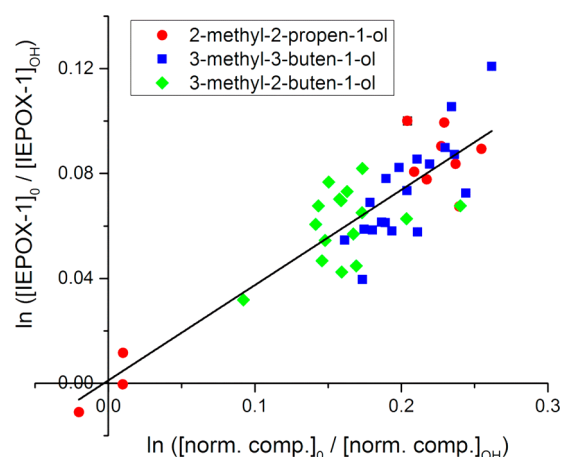

Figure 1. Relative rate constant determination for IEPOX-1.

rate constant of the competitor). Similar measurements were made with IEPOX-4 and the plot of the data collected is shown in Figure 2. The slope of the best fit line in Figure 2 is 0.371 ± 0.036, which corresponds to an IEPOX-4 + OH rate constant of $3.60 \pm 0.76 \times 10^{-11}$ cm^3 molecule^{-1} s^{-1}.
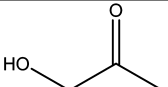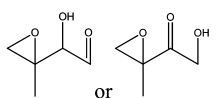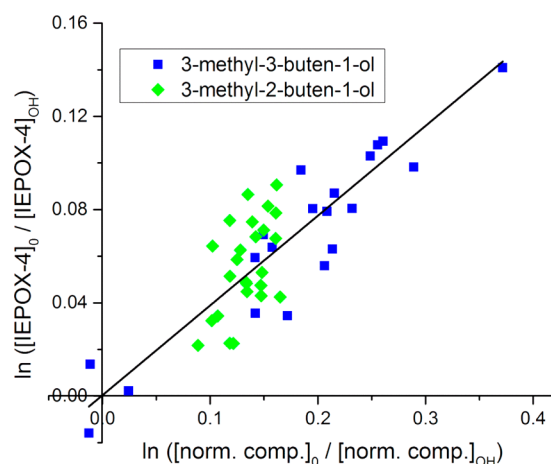

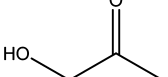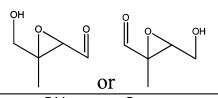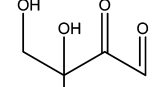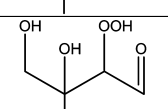**Figure 2.** Relative rate constant determination for IEPOX-4.

While estimates of the IEPOX + OH rate constants have previously been made, this work represents the first experimental determination of the OH rate constants for IEPOX-1 and IEPOX-4. Because these previous estimates have already been incorporated into atmospheric chemistry models, it is of interest to compare the new experimental results to the various available estimates. An upper bound to the IEPOX + OH rate constant has been previously estimated by Paulot et al. to be $k(T) = 5.78 \times 10^{-11} \exp(-400/T)$, or 1.5×10^{-11} cm^3 molecule^{-1} s^{-1} at 298 K.[14] Empirical structure−reactivity models have also been used to estimate the OH rate constants for both of the epoxides. The OH rate constant for IEPOX-1 was estimated to be 3.44×10^{-11} cm^3 molecule^{-1} s^{-1} by the EPIWEB database[34] (which is based on Kwok et al. formulation[35]) and 1.5×10^{-11} cm^3 molecule^{-1} s^{-1} by the Master Chemical Mechanism Version 3.2 (MCM v3.2).[36] Similar estimates for IEPOX-4 + OH rate constant are available from the same sources: 1.72×10^{-11} cm^3 molecule^{-1} s^{-1} and 0.9×10^{-11} cm^3 molecule^{-1} s^{-1} (from EPIWEB and MCM v3.2, respectively). Since about 90% of the experimentally measured

Table 1. Relative Product Yields for IEPOX-1 and IEPOX-4 Oxidation

m/z (MH$^+$)	deduced molecular species	relative yield without NO (%)	relative yield with NO (%)
	IEPOX-1		
75		78	81
117	or	22	19
	IEPOX-4		
61		12	14
75		24	25
89	$C_4H_8O_2$ or $C_3H_4O_3$	11	13
117	or	16	22
133		37	26
151			

OH rate constants used in the determination of the EPIWEB model fall within a factor of 2 of the actual experimentally determined rate constants,[35] the fact the newly determined experimental IEPOX + OH rate constants are within a factor of 2 of the EPIWEB predictions indicates that the EPIWEB model performed reasonably accurately in the prediction of these rate constants. Of course, the experimental rate constants have been determined to a much higher degree of precision and are likely to be much more reliable than the estimated EPIWEB values. On the other hand, the estimated IEPOX + OH rate constants currently incorporated into the MCM v3.2 model[36] and the Paulot et al. estimate[14] are considerably smaller than the newly determined experimental values.

To the best of our knowledge, OH rate constants have been experimentally determined for only 4 simple epoxides: ethylene oxide (1,2-epoxyethane, 0.95×10^{-13} cm^3 molecules^{-1} s^{-1}),[37] propylene oxide (1,2-epoxypropane, 4.95×10^{-13} cm^3 molecules^{-1} s^{-1}),[37] 1,2-epoxybutane (1.9×10^{-12} cm^3 molecules^{-1} s^{-1}),[38] and epichlorohydrin (1-chloro-2,3-epoxypropane, 3.93×10^{-13} cm^3 molecules^{-1} s^{-1}).[39] Compared to these relatively small OH reaction rate constants, it is apparent that the presence of neighboring hydroxy groups in the IEPOX compounds leads to significant greater OH reaction rate constants.

Product Study. Because the IEPOX species are saturated hydrocarbons, it is expected that they will react with OH via a hydrogen abstraction mechanism forming water as a coproduct. Both of the epoxide compounds have several different hydrogen atoms that could potentially be abstracted by the OH radical, thus there are several different possible reaction pathways. As described in the Experimental Section, the product species were identified by taking mass spectra with the OH source on and off, and then looking for new signals in the OH source in the PTR-CIMS spectrum. Because all of the predicted products contained hydroxy groups, they all were assumed to have equal PTR-CIMS response factors. Thus, the direct comparison of the relative signals was assumed to correspond to the molar relative product yields.

Table 1 shows the deduced product structures (based on the MH$^+$(H$_2$O)$_n$ signal carriers observed), with the specific isomers rationalized within the context of the overall mechanism, as discussed below), and relative product yields for IEPOX-1. For the C−C bond dissociation reaction types, there are two reaction products. However, due to mass coincidence complications, only one of the products was quantified via PTR-CIMS in each of the cases (these are the products listed in Table 1). From the structures of the products, a proposed mechanism for the formation of the products from IEPOX-1 was developed (Figure 3). Based on the products observed, it
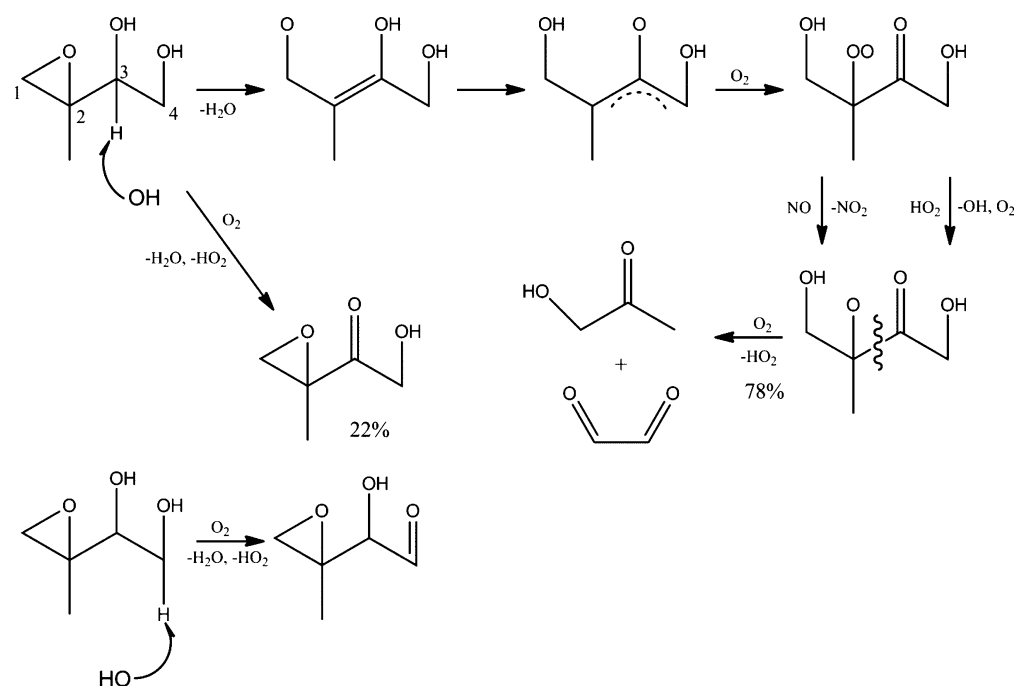
Figure 3. Gas phase OH-initiated oxidation mechanism for IEPOX-1 (NO-free product yields are given).

seems likely that the OH radical abstracts a hydrogen atom from either of the carbons with the hydroxy groups (C3 or C4). This supposition is also supported by the structure reactivity analysis given in the preceding section: neighboring hydroxy groups apparently lower the activation barrier for abstraction, which leads to preferential abstraction at these carbon atom sites (e.g., abstraction of hydrogen atoms from the epoxide carbon atom is too slow to compete) and to greater overall OH reaction rate constants. When the C4 hydrogen is abstracted (depicted in the lower part of Figure 3), reaction with O_2, then with either NO or HO_2, followed by reaction with O_2 will lead to the net result that this terminal hydroxy group is converted into an aldehyde group. However if the C3 hydrogen is abstracted, the resulting compound can either be converted into a ketone via reaction with O_2 (shown in the middle of Figure 3), or after a series of rearrangements and reactions similar to those occurring subsequent to the abstraction at the C4 site, the C2−C3 bond can split yielding hydroxyacetone and glyoxal (shown in the upper right portion of Figure 3). Because both the aldehyde and ketone species have the same m/z ratio, we cannot distinguish between the two possible products and note the total yield (in the absence of NO) of the two species is 22%, while the C2−C3 bond dissociation channel accounts for 78% of the total oxidation products for IEPOX-1. No hydroperoxide products (potentially arising from HO_2 reaction) were detected for IEPOX-1, and the NO dependence data suggests that the NO-free (presumably due to RO_2 and/or HO_2 reactions) and NO-present reaction mechanisms are similar. The mechanism currently incorporated into MCM v3.2 assumes that the isoprene backbone remains intact only when the C4 hydrogen is abstracted (i.e., it does not include a ketone formation channel).[36] For the bond dissociation channel, MCM v3.2 assumes that the bond breaking occurs at the C1−C2 bond. Because this channel is predicted to produce a one carbon and a four carbon product, and we observed m/z ratios consistent only with two, three, and five carbon products, we contend that the present results indicate the MCM v3.2

mechanism is not consistent with the experimental data. On the other hand, MCM v3.2 predicts that 28% of IEPOX-1 oxidation is carbon backbone-conserving and 72% of IEPOX-1 oxidation leads to fragmentation, which is in good agreement with the experimental results.

Table 1 and Figure 4 show the relative product yields and a possible mechanism for their formation for IEPOX-4 oxidation. As with IEPOX-1, the OH radical abstracts a hydrogen atom from either of the carbons with the hydroxy groups (C1 or C4). Abstraction from either C1 or C4 can result in the oxidation of the hydroxy group to an aldehyde group, and the total yield of these two potential species was found to be 16% (in the absence of NO). When a hydrogen atom is abstracted from C4, after a series of rearrangements and oxidations, a four oxygen intermediate is formed (shown in the upper right portion of Figure 4). The C2−C3 bond can break to form hydroxyacetone and glyoxal (24% yield), or the isoprene backbone can stay intact, forming a dihydroxy dicarbonyl species (37% yield). A possible hydroperoxide product (from HO_2 reaction) can also be formed from this channel, and because it has a MH^+ m/z value that is 18 mass units higher than the dihydroxy dicarbonyl species (which was detected as several hydrated MH^+ ions), the signal carrier at m/z 151 might be either or both species. In fact, the NO-dependence of this signal carrier does suggest that at least some of the signal may be due to a hydroperoxide product. When the C1 hydrogen is abstracted, a series of rearrangements and oxidations take place and eventually the C2−C3 bond breaks yielding hydroxyacetaldehyde and 2-oxopropanal (12% yield). A product with a molecular formula of likely either $C_4H_8O_2$ or $C_3H_4O_3$ is also observed (11% yield), but it could not be placed in the mechanism. Excluding the unknown species and accounting for the ambiguity in the exact mechanism of formation for the aldehyde species, the product yield data indicates that the C4 abstraction channel is the dominant product mechanism for IEPOX-4 oxidation. While MCM v3.2 does correctly anticipate that the C2−C3 bond dissociates in the formation of some reaction products for
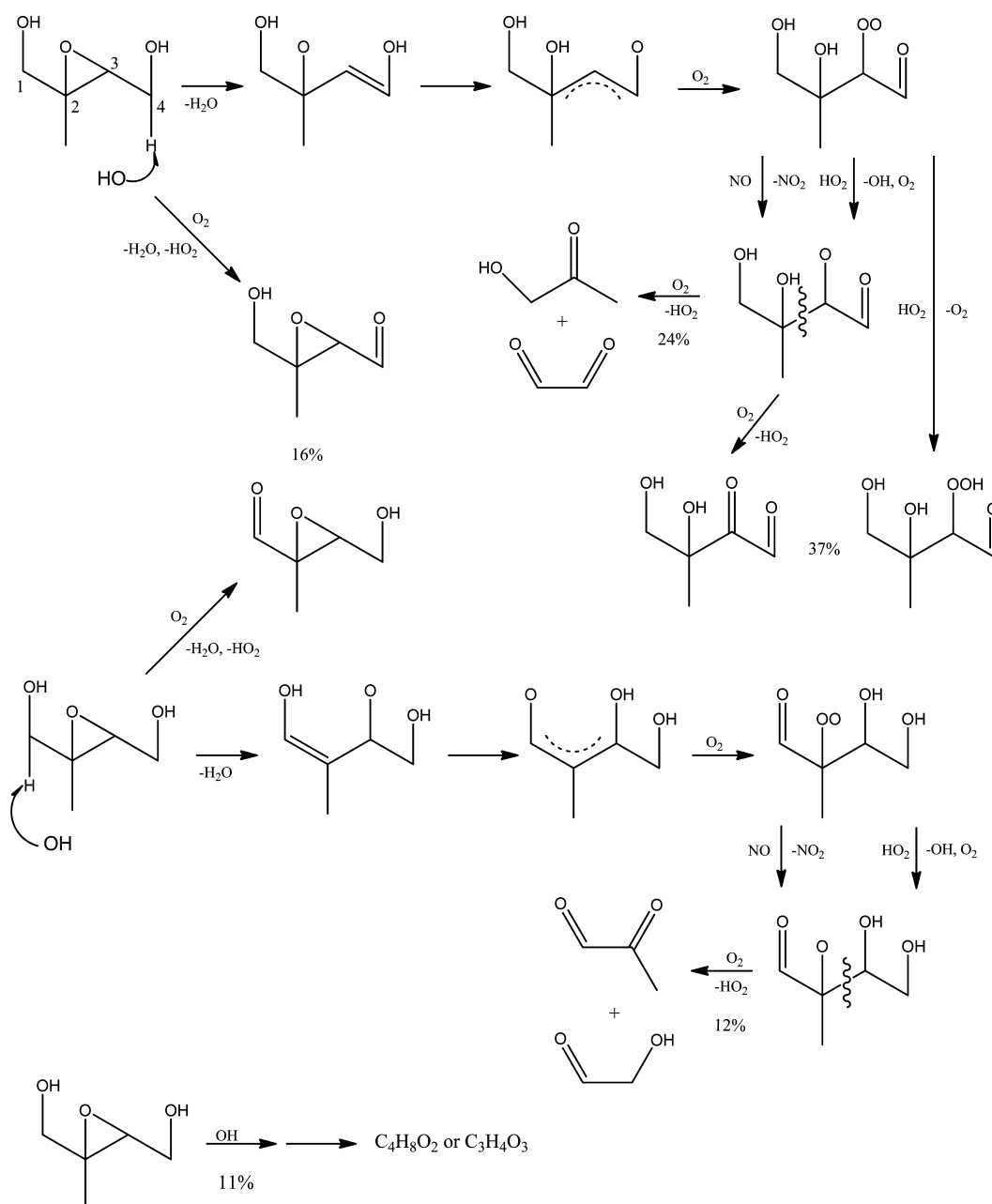
Figure 4. Gas phase OH-initiated oxidation mechanism for IEPOX-4 (NO-free product yields are given).

IEPOX-4, it supposes that the C1 and C4 abstraction pathways are exactly equally likely and the mechanism does not include an isoprene backbone-retaining aldehyde formation pathway.[36] These latter two mechanistic features of MCM v3.2 are at odds with the present experimental observations for IEPOX-4 oxidation.

Atmospheric Implications. Assuming a constant average OH concentration, gas phase process-only atmospheric lifetimes can be calculated from the newly obtained OH reaction rate constants. For an average OH concentration of 1×10^6 molecules cm^{-3}, both IEPOX compounds are calculated to have gas phase process-only lifetimes of about 8 h, whereas at the elevated OH concentrations found in isoprene-dominated environments (5×10^6 molecules cm^{-3}),[40,41] the gas phase process-only lifetimes are only about 1.5 h for both IEPOX compounds. Therefore, this traditional measure of VOC

reactivity suggests that IEPOX species can be quickly oxidized by gas phase processes initiated by the OH radical.

A more thorough analysis of the atmospheric fate of the IEPOX compounds has previously been modeled by Eddingsaas, et al.[22] The model examines three potential fates for the epoxides: gas phase oxidation, aerosol phase reaction, or dry deposition. In the case of the first two processes, the physical partitioning between the gas and aerosol phases must be considered, as well as the chemical reaction mechanisms that eventually lead to the permanent removal of the IEPOX species from the atmosphere. The partitioning of hydrophilic compounds like IEPOX into aqueous phase-like aerosols is governed by Henry's Law constant of the water-soluble organic compound:

12873

dx.doi.org/10.1021/es403340g | Environ. Sci. Technol. 2013, 47, 12868–12876

$$H_i^{\text{HL}} = \frac{c_{w,i}}{p_i} = \frac{A_i \gamma^{\text{HL}_i}}{M_i(\text{LWC})p_i} \qquad (7)$$

where H_i^{HL} is the Henry's Law constant of species i, $c_{w,i}$ is the aqueous phase concentration, p_i is the gas phase partial pressure of species i. A_i represents the aerosol phase concentration, M_i is the molecular weight, γ^{HL_i} is the activity coefficient of compound i in the aqueous mixture (assumed to be 1) and LWC is the liquid water content. Based on structure reactivity model predictions and comparison to similar compounds, Eddingsaas et al. estimated the IEPOX Henry's law constant to be $H^{\text{HL}} = 1.3 \times 10^8$ M atm^{-1}. The ratio of the amount of IEPOX in the aerosol phase as compared to the gas phase (A_i/p_i) is obtained by rearranging eq 7. Eddingsaas et al. found that the fraction of epoxide in the aerosol to that in the gas phase varies from 0.003 to 0.03 to 0.25 for LWC values of 1, 10, and 100 μg m^{-3}, respectively. However, this calculation represents the expected equilibrium partitioning of IEPOX compounds between the gas and aerosol phases in the absence of chemical reaction processes. For example, relatively fast gas phase oxidation chemistry as compared to the rate of aerosol phase hydrolysis chemistry would lead to a larger fraction of IEPOX being removed by gas phase processes than the physical partitioning model predicts.

At the time that the Eddingsaas et al. paper was published, neither the actual OH + IEPOX nor IEPOX hydrolysis rate constants had been experimentally determined. Thus, estimates of both rate constants were used to model the chemical reaction processes: the OH + IEPOX rate constant was estimated from the Paulot et al. upper limit cited above (1.5 × 10^{-11} cm^3 molecule^{-1} s^{-1})[14] and the IEPOX hydrolysis rate constant was assumed to have the same value as the 1,4-dihydroxy-2,3-epoxybutane hydrolysis rate constant (0.05 M^{-1} s^{-1}).[22] In addition to these chemical reaction rate constants, the dry deposition rate constant was assumed to be 2.5 × 10^{-5} s^{-1}. As part of the initial conditions used for the Eddingsaas model, an OH radical concentration of 5 × 10^6 molecules cm^{-3} was assumed.[22] The Eddingsaas model was implemented using the kinetics simulation software Kintecus[42] for 20 h. The LWC was set to either 10 or 100 μg m^{-3} and the pH was set to either 2 or 4. Using the estimated rate constants, at a pH of 4 and a LWC of 10 μg m^{-3}, less than 1% of the IEPOX was predicted to form ring-opened products in the aerosol phase; however, at a pH of 2, the yield approached 15%. With high aerosol liquid water content (100 μg m^{-3}), the Eddingsaas et al. model indicated that gas phase oxidation and dry deposition still dominated at a pH of 4 (<2% of IEPOX fate was reaction in the aerosol phase), whereas at a pH of 2, greater than 50% of IEPOX formed ring-opening products in the aerosol phase. Thus, Eddingsaas et al. found that the gas phase OH reaction dominated the fate of IEPOX at all conditions except for those of high acidity (pH 2) and high LWC (100 μg m^{-3}), where the aerosol phase processes were found to dominate.

With the measurement of the OH + IEPOX gas phase rate constants reported in the present work (3.52 × 10^{-11} cm^3 molecule^{-1} s^{-1} for IEPOX-1 and of 3.60 × 10^{-11} cm^3 molecule^{-1} s^{-1} for IEPOX-4), and our laboratory's recent measurements of the acid-catalyzed IEPOX hydrolysis rate constants for the aerosol phase reactions (0.0079 M^{-1} s^{-1} for IEPOX-1 and 0.036 M^{-1} s^{-1} for IEPOX-4),[17] it is now possible to use the Eddingsaas et al. framework to predict much more accurate atmospheric fates for the isomer-specific IEPOX compounds. Except for these chemical reaction kinetics

parameters, all other parameters used in the Eddingsaas et al. work were held at the same values for the present model calculations. The results from the model using the IEPOX-1-specific OH gas phase oxidation and aerosol phase hydrolysis rate constants and the results from the model using IEPOX-4-specific rate constants are presented in Table 2. Since the

Table 2. Model Calculated Atmospheric Fates of IEPOX-1 and IEPOX-4 (See Text for Discussion of Model and Parameters)

aerosol properties	aerosol phase reaction (%)	gas phase oxidation (%)	dry deposition (%)
	IEPOX-1		
LWC: 10 μg m^{-3}, pH: 4	0.01	87.6	12.4
LWC: 10 μg m^{-3}, pH: 2	1.2	86.6	12.2
LWC: 100 μg m^{-3}, pH: 4	0.1	87.5	12.4
LWC: 100 μg m^{-3}, pH: 2	8.7	80.0	11.3
	IEPOX-4		
LWC: 10 μg m^{-3}, pH: 4	0.05	88.2	11.8
LWC: 10 μg m^{-3}, pH: 2	5.0	83.7	11.2
LWC: 100 μg m^{-3}, pH: 4	0.4	87.8	11.7
LWC: 100 μg m^{-3}, pH: 2	29.0	62.6	8.4

experimental gas phase OH rate constants used in the present model calculations are larger than the value used previously and the experimental IEPOX aerosol phase hydrolysis rate constants used in the present model calculations are smaller than the value used previously, it is not surprising that that the present model calculations indicate that gas phase OH reaction is more dominant in the fate of atmospheric IEPOX than did the previous model calculations of Eddingsaas et al.[22] In particular, while the estimations used in the Eddingsaas model showed the aerosol phase reaction dominating the fate of IEPOX at high LWC and low pH, the current model calculations show that gas phase oxidation dominates at all LWC and pH values investigated. For example, the current model calculations predict that for a pH of 2 and LWC of 100 μg m^{-3}, only 8.7% of IEPOX-1 and 29% of IEPOX-4 is expected to undergo aerosol phase reaction. For identical aerosol conditions, the Edingsaas et al. model predicted that 52% of IEPOX is expected to undergo aerosol phase reaction. Therefore, the present results indicate that higher LWC (>100 μg m^{-3}) and/or lower pH (<2) conditions would need to be present in ambient aerosols in order for aerosol phase reaction to be the dominant fate of IEPOX compounds.

The finding that gas phase OH chemistry may be more important than previously estimated suggests that IEPOX may play a significant role in gas phase chemistry (i.e., ozone formation, and NO$_x$ processing). Since the present work found a number of qualitative and quantitative differences in the gas phase product mechanism as compared to the current IEPOX chemistry represented in MCM v3.2, it will be important to update such models in the effort to better model isoprene's overall role in gas phase chemical processes. It is also the case that some of the species that are produced in the gas phase oxidation of IEPOX are known to be important to SOA

formation (such as glyoxal[1−3]), such that *gas phase* IEPOX reaction chemistry may ultimately significantly contribute to the *aerosol phase* constituents of isoprene-derived SOA.

■ ASSOCIATED CONTENT

Ⓢ Supporting Information

Details on various experimental procedures and a derivation. This material is available free of charge via the Internet at http://pubs.acs.org.

■ AUTHOR INFORMATION

Corresponding Author

*E-mail: matthew.elrod@oberlin.edu.

Notes

The authors declare no competing financial interest.

■ ACKNOWLEDGMENTS

■ REFERENCES

(1) Carlton, A. G.; Wiedinmyer, C.; Kroll, J. H. A review of secondary organic aerosol (SOA) formation from isoprene. *Atmos. Chem. Phys.* **2009**, *9*, 4987−5005.

(2) Hallquist, M.; Wenger, J. C.; Baltensperger, U.; Rudich, Y.; Simpson, D.; Claeys, M.; Dommen, J.; Donahue, N. M.; George, C.; Goldstein, A. H.; Hamilton, J. F.; Herrmann, H.; Hoffmann, T.; Iinuma, Y.; Jang, M.; Jenkin, M. E.; Jimenez, J. L.; Kiendler-Scharr, A.; Maenhaut, W.; McFiggans, G.; Mentel, T. F.; Monod, A.; Prevot, A. S. H.; Seinfeld, J. H.; Surratt, J. D.; Szmigielski, R.; Wildt, J. The formation, properties and impact of secondary organic aerosol: Current and emerging issues. *Atmos. Chem. Phys.* **2009**, *9*, 5155−5236.

(3) Ervens, B.; Turpin, B. J.; Weber, R. J. Secondary organic aerosol formation in cloud droplets and aqueous particles (aqSOA): A review of laboratory, field and model studies. *Atmos. Chem. Phys.* **2011**, *11*, 11069−11102.

(4) Guenther, A.; Karl, T.; Harley, P.; Wiedinmyer, C.; Palmer, P. I.; Geron, C. Estimates of global terrestrial isoprene emissions using MEGAN (model of emissions of gases and aerosols from nature). *Atmos. Chem. Phys.* **2006**, *6*, 3181−3210.

(5) Chan, M. N.; Surratt, J. D.; Claeys, M.; Edgerton, E. S.; Tanner, R. L.; Shaw, S. L.; Zheng, M.; Knipping, E. M.; Eddingsaas, N. C.; Wennberg, P. O.; Seinfeld, J. H. Characterization and quantification of isoprene-derived epoxydiols in ambient aerosol in the southeastern United States. *Environ. Sci. Technol.* **2010**, *44*, 4590−4596.

(6) Claeys, M.; Graham, B.; Vas, G.; Wang, W.; Vermeylen, R.; Pashynska, V.; J., C.; Guyon, P.; Andreae, M. O.; Artaxo, P.; Maenhaut, W. Formation of secondary organic aerosols through photooxidation of isoprene. *Science* **2004**, *303*, 1173−1176.

(7) Wang, W.; Kourtchev, I.; Graham, B.; Cafmeyer, J.; Maenhaut, W.; Claeys, M. Characterization of oxygenated derivatives of isoprene related to 2-methyltetrols in Amazonian aerosols using trimethylsilylation and gas chromatography/ion trap mass spectrometry. *Rapid Commun. Mass Spectrom.* **2005**, *19*, 1343−1351.

(8) Surratt, J. D.; Lewandowski, M.; Offenberg, J. H.; Jaoui, M.; Kleindienst, T. E.; Edney, E. O.; Seinfeld, J. H. Effect of acidity on secondary organic aerosol formation from isoprene. *Environ. Sci. Technol.* **2007**, *41*, 5363−5369.

(9) Altieri, K. E.; Turpin, B. J.; Seitzinger, S. P. Oligomers, organosulfates, and nitrooxy organosulfates in rainwater identified by ultra-high resolution electrospray ionization FT-ICR mass spectrometry. *Atmos. Chem. Phys.* **2009**, *9*, 2533−2542.

(10) Gómez-González, Y.; Surratt, J. D.; Cuyckens, F.; Szmigielski, R.; Vermeylen, R.; Jaoui, M.; Lewandowski, M.; Offenberg, J. H.; Kleindienst, T. E.; Edney, E. O.; Blockhuys, F.; Van Alsenoy, C.; Maenhaut, W.; Claeys, M. Characterization of organosulfates from the photooxidation of isoprene and unsaturated fatty acids in ambient aerosol using liquid chromatography/(−) electrospray ionization mass spectrometry. *J. Mass Spectrom.* **2008**, *43*, 371−382.

(11) Surratt, J. D.; Gómez-González, Y.; Chan, A. W. H.; Vermeylen, R.; Shahgholi, M.; Kleindienst, T. E.; Edney, E. O.; Offenberg, J. H.; Lewandowski, M.; Jaoui, M.; Maenhaut, W.; Claeys, M.; Flagan, R. C.; Seinfeld, J. H. Organosulfate formation in biogenic secondary organic aerosol. *J. Phys. Chem. A* **2008**, *112*, 8345−8378.

(12) Hatch, L. E.; Creamean, J. M.; Ault, A. P.; Surratt, J. D.; Chan, M. N.; Seinfeld, J. H.; Edgerton, E. S.; Su, Y.; Prather, K. A. Measurements of isoprene-derived organosulfates in ambient aerosols by aerosol time-of-flight mass spectrometry—Part 1: Single particle atmospheric observations in Atlanta. *Environ. Sci. Technol.* **2011**, 110523130843049.

(13) Lin, Y.-H.; Zhang, Z.; Docherty, K. S.; Zhang, H.; Budisulistiorini, S. H.; Rubitschun, C. L.; Shaw, S. L.; Knipping, E. M.; Edgerton, E. S.; Kleindienst, T. E.; Gold, A.; Surratt, J. D. Isoprene epoxydiols as precursors to secondary organic aerosol formation: Acid-catalyzed reactive uptake studies with authentic compounds. *Environ. Sci. Technol.* **2012**, *46*, 250−258.

(14) Paulot, F.; Crounse, J. D.; Kjaergaard, H. G.; Kurten, A.; St. Clair, J. M.; Seinfeld, J. H.; Wennberg, P. O. Unexpected epoxide formation in the gas-phase photooxidation of isoprene. *Science* **2009**, *325*, 730−733.

(15) Darer, A. I.; Cole-Filipiak, N. C.; O'Connor, A. E.; Elrod, M. J. Formation and stability of atmospherically relevant isoprene-derived organosulfates and organonitrates. *Environ. Sci. Technol.* **2011**, *45*, 1895−1902.

(16) Hu, K. S.; Darer, A. I.; Elrod, M. J. Thermodynamics and kinetics of the hydrolysis of atmospherically relevant organonitrates and organosulfates. *Atmos. Chem. Phys.* **2011**, *11*, 8307−8320.

(17) Cole-Filipiak, N. C.; O'Connor, A. E.; Elrod, M. J. Kinetics of the hydrolysis of atmospherically relevant isoprene-derived hydroxy epoxides. *Environ. Sci. Technol.* **2010**, *44*, 6718−6723.

(18) Surratt, J. D.; Chan, A. W. H.; Eddingsaas, N. C.; Chan, M.; Loza, C. L.; Kwan, A. J.; Hersey, S. P.; Flagan, R. C.; Wennberg, P. O.; Seinfeld, J. H. Reactive intermediates revealed in secondary organic aerosol formation from isoprene. *Proc. Natl. Acad. Sci.* **2010**, *107*, 6640−6645.

(19) Lin, Y.-H.; Zhang, H.; Pye, H. O. T.; Zhang, Z.; Marth, W. J.; Park, S.; Arashiro, M.; Cui, T.; Budisulistiorini, S. H.; Sexton, K. G.; Vizuete, W.; Xie, Y.; Luecken, D. J.; Piletic, I. R.; Edney, E. O.; Bartolotti, L. J.; Gold, A.; Surratt, J. D. Epoxide as a precursor to secondary organic aerosol formation from isoprene photooxidation in the presence of nitrogen oxides. *Proc. Natl. Acad. Sci.* **2013**, *110*, 6718−6723.

(20) Budisulistiorini, S. H.; Canagaratna, M. R.; Croteau, P. L.; Marth, W. J.; Baumann, K.; Edgerton, E. S.; Shaw, S. L.; Knipping, E. M.; Worsnop, D. R.; Jayne, J. T.; Gold, A.; Surratt, J. D. Real-yime continuous characterization of secondary organic aerosol derived from isoprene epoxydiols in downtown Atlanta, Georgia, using the Aerodyne Aerosol Chemical Speciation Monitor. *Environ. Sci. Technol.* **2013**, *47*, 5686−5694.

(21) Hatch, L. E.; Creamean, J. M.; Ault, A. P.; Surratt, J. D.; Chan, M. N.; Seinfeld, J. H.; Edgerton, E. S.; Su, Y.; Prather, K. A. Measurements of isoprene-derived organosulfates in ambient aerosols by aerosol time-of-flight mass spectrometry—Part 2: Temporal variability and formation mechanisms. *Environ. Sci. Technol.* **2011**, *45*, 8648−8655.

(22) Eddingsaas, N. C.; VanderVelde, D. G.; Wennberg, P. O. Kinetics and products of the acid-catalyzed ring-opening of atmospherically relevant butyl epoxy alcohols. *J. Phys. Chem. A* **2010**, *114*, 8106−8113.

(23) Harwood, L. M. A simple laboratory procedure for preparation of (1-methylethenyl)oxirane (3,4-epoxyisoprene). *Synth. Commun.* **1990**, *20*, 1287−1290.

(24) Zhang, Z.; Lin, Y. H.; Zhang, H.; Surratt, J. D.; Ball, L. M.; Gold, A. Technical note: Synthesis of isoprene atmospheric oxidation products: Isomeric epoxydiols and the rearrangement cis and trans-3-

methyl-3,4-dihydroxytetrahydrofuran. *Atmos. Chem. Phys.* **2012**, *12*, 8529−8535.

(25) Shepard, A. F.; Johnson, J. R. Rearrangement of unsaturated 1,4-glycols. 2-methyl-2-butene-1,4-diol. *J. Am. Chem. Soc.* **1932**, *54*, 4385−4391.

(26) Elrod, M. J. Kinetics study of the aromatic bicyclic peroxy radical + NO reaction: Overall rate constant and nitrate product yield measurements. *J. Phys. Chem. A* **2011**, *115*, 8125−8130.

(27) National Institute of Standards and Technology, Chemical Kinetics Database. http://kinetics.nist.gov/kinetics/index.jsp (accessed 7/12/13).

(28) Yeung, L. Y.; Elrod, M. J. Experimental and computational study of the kinetics of the OH + pyridine and its methyl- and ethyl-substituted derivatives. *J. Phys. Chem. A* **2003**, *107*, 4470−4477.

(29) Bierbaum, V. M.; DePuy, C. H.; Shapiro, R. H.; Stewart, J. H. Flowing afterglow studies of the reactions of hydroxide, amide, and methoxide ions with ethylene oxide and propylene oxide. *J. Am. Chem. Soc.* **1976**, *98*, 4229−4235.

(30) Seeley, J. V.; Meads, R. F.; Elrod, M. J.; Molina, M. J. Temperature and pressure dependence of the rate constant for the HO_2 + NO reaction. *J. Phys. Chem.* **1996**, *100*, 4026−4031.

(31) Montenegro, A.; Ishibashi, J. S. A.; Lam, P.; Li, Z. Kinetics study of reactions of α-pinene and β-pinene with hydroxyl radical at 1−8 Torr and 240−340 K using the relative rate/discharge flow/mass spectrometry method. *J. Phys. Chem. A* **2012**, *116*, 12096−12103.

(32) Birdsall, A. W.; Andreoni, J. F.; Elrod, M. J. Investigation of the role of bicyclic peroxy radicals in the oxidation mechanism of toluene. *J. Phys. Chem. A* **2010**, *114*, 10655−10663.

(33) Cometto, P. M.; Dalmasso, P. R.; Taccone, R. l. A.; Lane, S. I.; Oussar, F. t.; Daële, V. r.; Mellouki, A.; Bras, G. L. Rate coefficients for the reaction of OH with a series of unsaturated alcohols between 263 and 371 K. *J. Phys. Chem. A* **2008**, *112*, 4444−4450.

(34) Environmental Protection Agency, EPIWEB 4.0, http://www.epa.gov/opptintr/exposure/pubs/episuitedl.htm.

(35) Kwok, E. S. C.; Atkinson, R. Estimation of hydroxyl radical reaction rate constants for gas-phase organic compounds using a structure-reactivity relationship: An update. *Atmos. Environ.* **1995**, *29*, 1685−1695.

(36) Saunders, S. M.; Jenkin, M. E.; Derwent, R. G.; Pilling, M. J. Protocol for the development of the Master Chemical Mechanism, MCM v3 (Part A): Tropospheric degradation of non-aromatic volatile organic compounds. *Atmos. Chem. Phys.* **2003**, *3*, 161−180.

(37) Wallington, T. J.; Liu, R.; Dagaut, P.; Kurylo, M. J. The gas phase reactions of hydroxyl radicals with a series of aliphatic ethers over the temperature range 240−440 K. *Int. J. Chem. Kinet.* **1988**, *20*, 41−49.

(38) Wallington, T. J.; Dagaut, P.; Kurylo, M. J. Correlation between gas-phase and solution-phase reactivities of hydroxyl radicals towards saturated organic compounds. *J. Phys. Chem.* **1988**, *92*, 5024−5028.

(39) Orkin, V. L.; Khamaganov, V. G.; Kozlov, S. N.; Kurylo, M. J. Measurements of rate constants for the OH reactions with bromoform ($CHBr_3$), $CHBr_2Cl$, $CHBrCl_2$, and epichlorohydrin (C_3H_5ClO). *J. Phys. Chem. A* **2013**, *117*, 3809−3818.

(40) Karl, T.; Guenther, A.; Turnipseed, A.; Tyndall, G.; Artaxo, P.; Martin, S. Rapid formation of isoprene photo-oxidation products observed in Amazonia. *Atmos. Chem. Phys.* **2009**, *9*, 7753−7767.

(41) Lelieveld, J.; Butler, T. M.; Crowley, J. N.; Dillon, T. J.; Fischer, H.; Ganzeveld, L.; Harder, H.; Lawrence, M. G.; Martinez, M.; Taraborrelli, D.; Williams, J. Atmospheric oxidation capacity sustained by a tropical forest. *Nature* **2008**, *452*, 737−740.

(42) Ianni, J. C., Kintecus, Windows Version 2.80, 2002. http://www.kintecus.com.